Predicting bulk powder flow dynamics in a continuous mixer operating in transitory regimes

C. Ammarcha [a], C. Gatumel [a], J.L. Dirion [a], M. Cabassud [b], V. Mizonov [c], H. Berthiaux [a,*]

[a] Université de Toulouse, EMAC, Centre RAPSODEE, UFR 3213 CNRS, Campus Jarlard, route de Teillet, F-81000 Albi, France
[b] Université de Toulouse, INPT, UPS, Laboratoire de Génie Chimique, UMR 5503 CNRS-, 4 allée Emile Monso, F-31432 Toulouse, France
[c] Ivanovo State Power Engineering University, Department of Applied Mathematics, Rabfakoskaya 34, 153003 Ivanovo, Russia

Keywords:
Powder mixing
Transitory regime
Continuous mixing
Markov chain
Stochastic process

A B S T R A C T

Over recent years there has been increasing interest in continuous powder mixing processes, due mainly to the development of on-line measurement techniques. However, our understanding of these processes remains limited, particularly with regard to their flow and mixing dynamics. In the present work, we study the behaviour of a pilot-scale continuous mixer during transitory regimes, in terms of hold-up weight and outflow changes. We present and discuss experimental results concerning the start-up dynamics of a Gericke GCM 500 mixer, for which a specific experimental protocol has been developed to determine the evolution of the hold-up in the mixer and the real outflow. Empirical relationships are derived so as to link hold-up weight variations with operating conditions. A simple stochastic approach, based on a non-homogeneous Markov chain, is developed to simulate the bulk particle flow and transport in the continuous mixer at a macroscopic level. Although this simple model is only based on the start-up behaviour, it provides a full description of the mixer dynamics in response to strong perturbations on the flow rate or on the rotational speed of the stirring device, such as negative or positive steps. This model is validated experimentally for a wide range of operating conditions, and constitutes a first approach to process control.

1. Introduction

The mixing of solids is a common operation in several industrial applications, such as pharmaceuticals, food, cements or powdered metal injection-molding. The operation aims to ensure a maximum added value and consistent homogeneity for both intermediate and finished products. Although most unit operations involved in the production process are continuous, the most prevalent process configuration used in industry today for powder mixing is still the batch process. One of the various reasons for this is the fact that relatively few continuous mixers are actually available on the market. Another explanation is related to the increasing multiplicity of formulations leading to the disputable conclusion that "the batch is the simplest way". In fact, the truth is that chemical engineering concepts still have difficulty gaining acceptance in these sectors, so there is always a sort of mystical attraction towards the "pot" in which the mixture is prepared. In the last decade, the implementation capability of continuous mixers in industry has consistently improved through the development of on-line and real-time techniques to assess the homogeneity of the mixtures, such as image analysis, NIR and Raman spectroscopy, or electrical methods like capacitance measurements. These techniques allow the development of standards for product quality and specification, and are in direct correspondence with the Process Analytical Technology (PAT) guidelines in the pharmaceutical industry. In recent years, continuous powder mixing has started to receive special attention from both industrial and academic quarters [1,2], resulting in greater interest in how to approach powder flow and mixing dynamics. But before working on a mixing model for different flows, investigations must obviously begin by studying the bulk powder flow dynamics of "pure" products, and by analysing the effect on the flow of powder characteristics, as well as the sensitivity of the system to process variables.

Understanding how a continuous mixer behaves during the transitory phases that are likely to occur when starting and emptying the mixer or re-loading the feeders is crucial for the control of the process and its industrial implementation. Equally important is our understanding of behaviour during changes in operating variables, such as the stirrer's rotational speed or the mass flow rates. It is worth noting that these transitory phases will have a strong effect on the variation of the hold-up weight in the mixer and consequently on the mean residence time of the powder, in turn affecting the quality of the mixtures. Very little experimental work

* Corresponding author.
E-mail address: henri.berthiaux@enstimac.fr (H. Berthiaux).

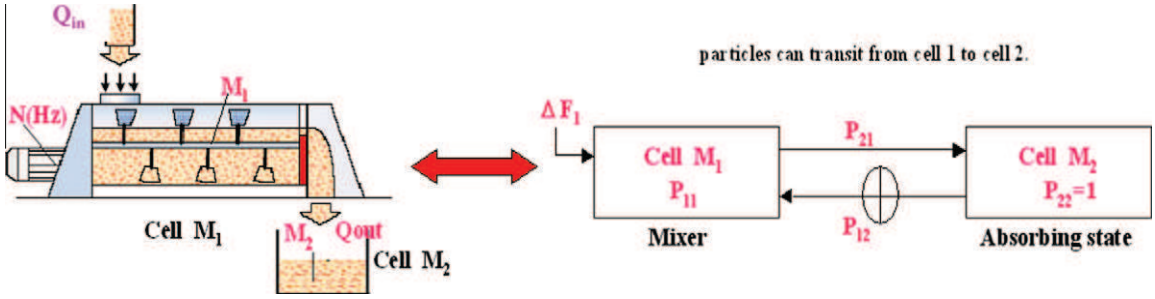

Fig. 1. Simple Markov chain representation of the continuous mixing process.

Fig. 2. Pilot scale continuous mixer Gericke GCM 500 used in the present work: loss-in-weight feeders (1,2); feeding chute tube (3); mixer outlet (4); balances (5,6).

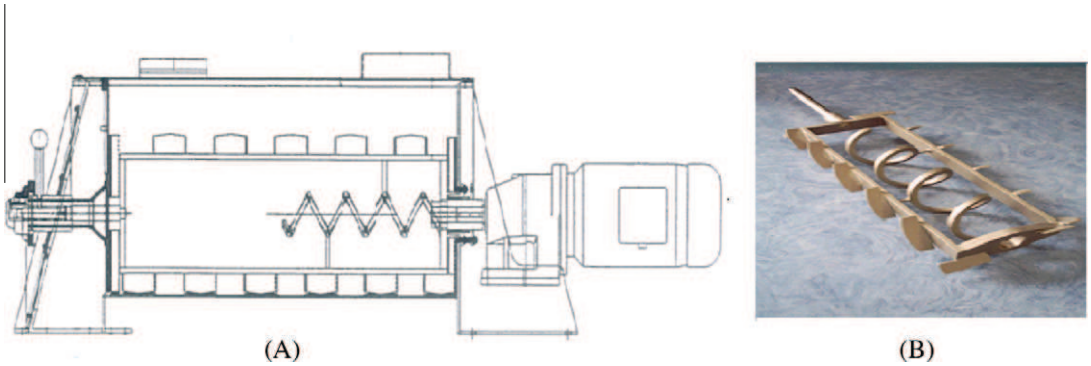

Fig. 3. Details of mixing system (A) and stirring device (B).

concerning transitory operation of continuous powder equipment has been reported in the literature so far. Markley and Puri [3], and then Sudah et al. [4] investigated the discharge process of batch bins under different rotational speeds of the tumbler from a purely experimental viewpoint. Spurling et al. [5] studied granular flow in a rotating cylinder, accounting for step changes in feed rate, axis inclination or rotational speed of the tumbler. They developed a mechanistic model of the particulate media flow dynamics based on a non-linear partial differential equation of the bulk flow motion.

In one of our works [6], we examined the effect of process disturbance, such as that occurring during periods of feeding of loss-in-weight feeders. In particular, we quantified the response of the mixer to filling sequences of two critical feeders in terms

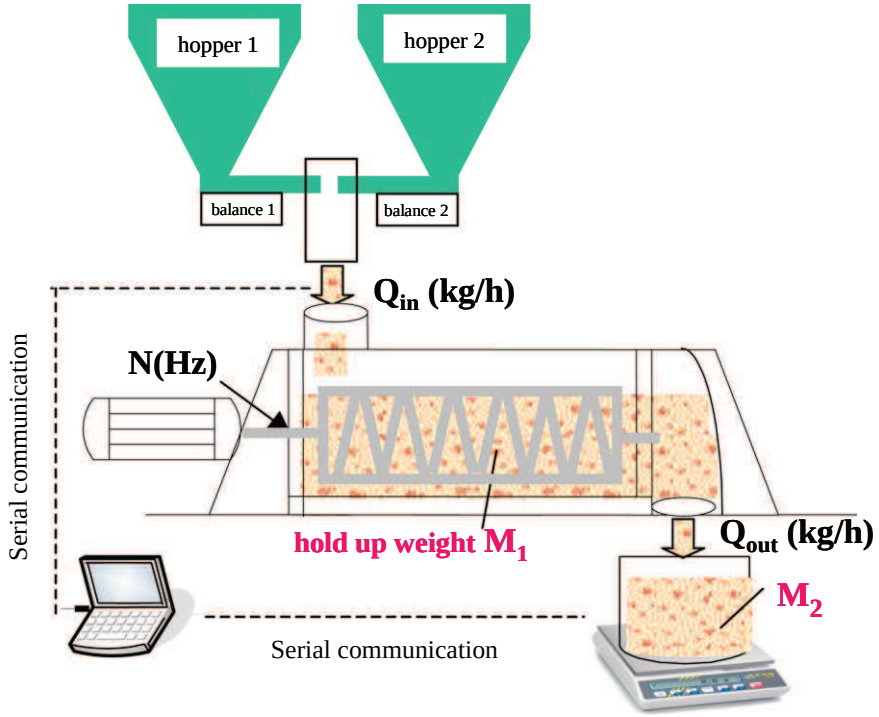

Fig. 4. Indirect measurement of the hold-up weight inside the mixer.

Table 1
Physical characteristics of the couscous particles used. Particle sizes (d_{10}, d_{50}, d_{90}) were obtained by sieving; true density obtained by Helium pycnometer; tapped density by a volumenometer. The Carr index is a ratio formed by aerated and tapped densities.

d_{50} (μm)	d_{10} (μm)	d_{90} (μm)	True density (g cm^{-3})	Tapped density (g cm^{-3})	Carr index (%)
1700	1375	1900	1.45	0.78	2.22

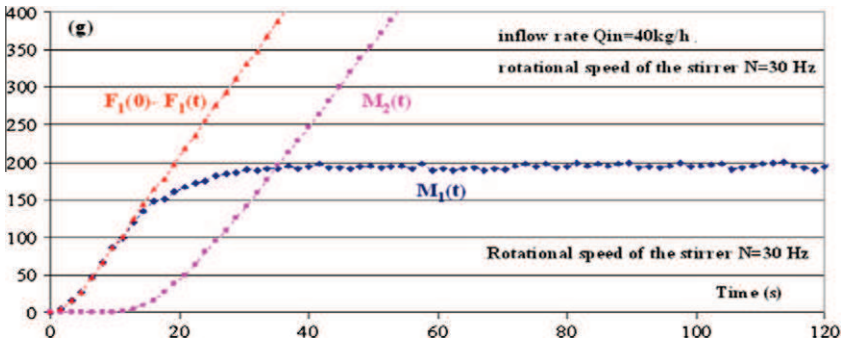

Fig. 5. Experimental evolution of the hold-up weight in the mixer during start-up.

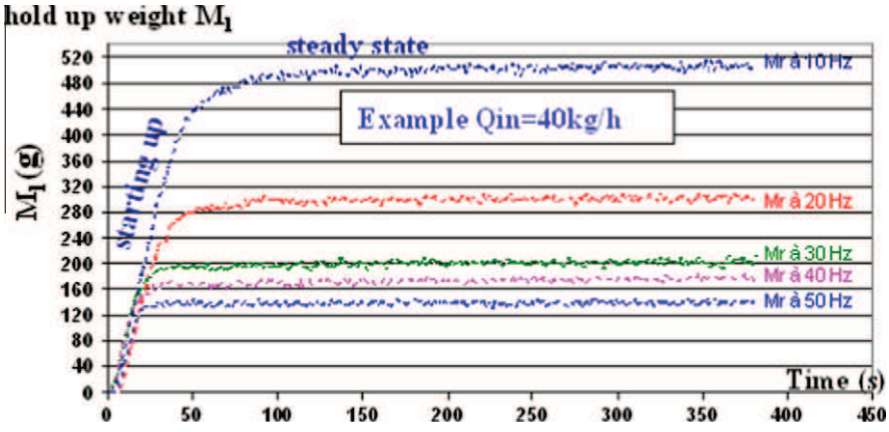

Fig. 6. Experimental evolution of hold-up weight for different rotational speeds of the stirrer.

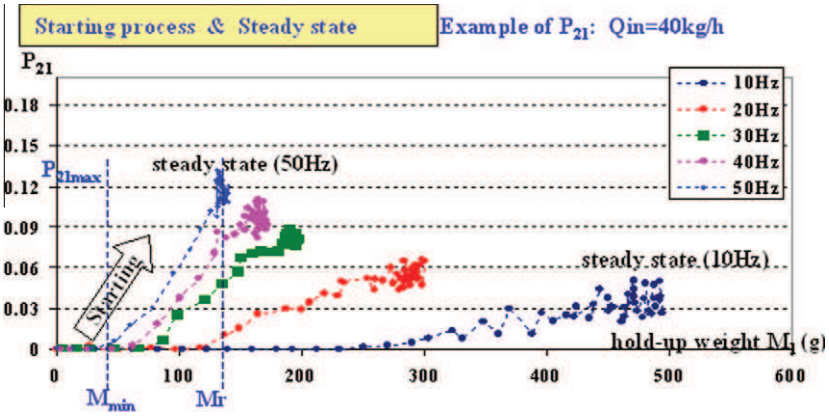

Fig. 7. Evolution of the probability P_{21} during start-up for the studied range of rotational speeds and $Q = 40$ kg h^{-1}.

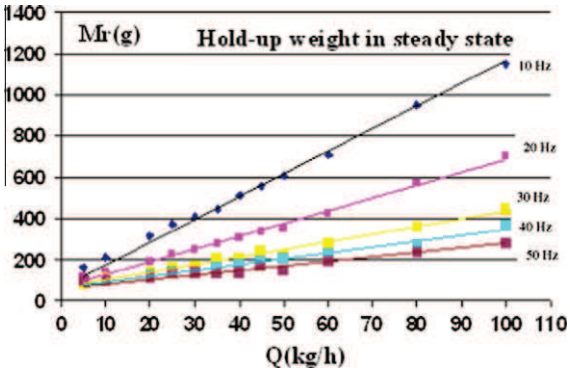

Fig. 8. Hold-up weight vs flowrate steady-state chart.

of mixture homogeneity. It was noted that it would actually be preferable to stop the process during these transitory periods, which is undoubtedly a critical aspect from an industrial standpoint. More recently [7], we investigated the emptying process of a continuous mixer and identified relationships between hold-up weight, outflow rate and process variables. A simple Markov chain was proposed to serve as a general modelling framework. In this paper we aim to extend our investigations into the transitory regime from both the theoretical and the practical point of view, so as to reach a better understanding of the flow dynamics. For this, we will primarily focus on the starting of the process and try to describe the dynamics of mixer filling, which has never been reported elsewhere. We will then investigate the effect of strong changes in the operating conditions that may need to be made while processing, such as step variations in the rotational speed of the stirrer.

2. A simple Markov chain representation of continuous mixing

In this section, we will build a simple Markov chain model to describe the macroscopic behaviour of particle flow, in terms of hold-up weight and outflow rate, in both steady and unsteady state operation of a continuous mixer. This first step aims to provide a general framework to the modelling of the process, keeping in mind the objective of being able to control the mixer in real-time. Going into more detail about the particulate flow inside the mixer will require at least a mesoscopic cell-model, and probably a microscopic representation through Distinct Element Modelling (DEM) to account for particle segregation, which is clearly beyond the objectives of the present work. It is also worth noting that

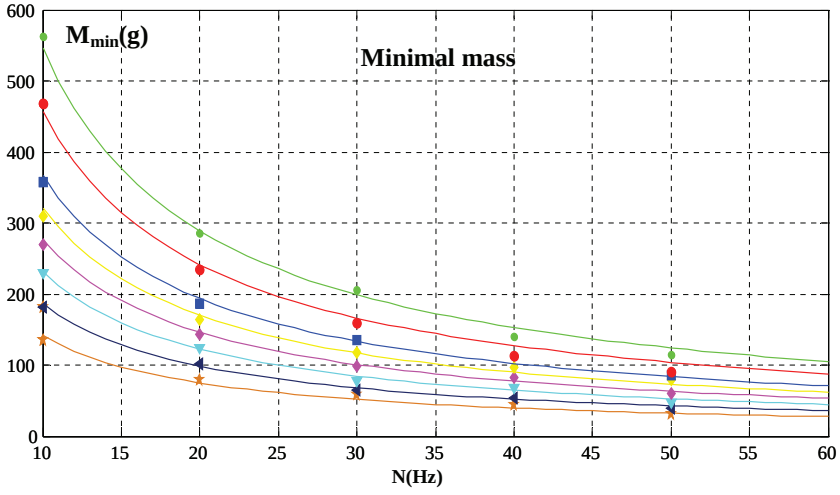

Fig. 9. Determination of an empirical relation for the minimum hold-up weight with the operating variables. Inflow rates are (from bottom to top): 10, 20, 30, 40, 50 60, 80 and 100 kg h^{-1}.

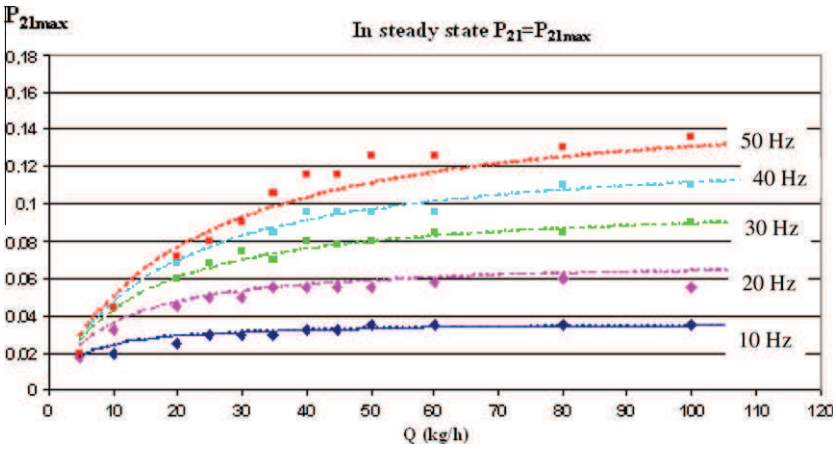

Fig. 10. Determination of an empirical relation for P_{21max} with the operating variables.

other types of modelling strategies, like integro-differential ones [8], may be used for particulate flow representation. Two reasons make these less valid than the Markov chain. First, experimental observation through Positron Emission Particle Tracking (PEPT) revealed evidence that the flow structure is not continuous, but closer to a tanks-in-series with internal recirculation configuration. Secondly, these modelling tools ultimately need an empirical determination of a diffusion-like coefficient, taken as a constant value, while this most probably depends on the flow rate.

The essence of a Markov chain model is that if the initial state (or present state) of a system is known and if the probabilities to transit to other states are also given, then it is possible to predict the future state of the system. Most of the time, the system under observation is a particle (or a fluid element in Residence Time Distribution issues), states are space locations and the problem is represented by a matrix formulation through a transition matrix P that collects the transition probabilities from state to state. For a complete description of Markov chains and their applications in powder technology, one may refer to our review paper [9].

Let us represent the entire mixer as being a single state (or cell), regardless of its level of homogeneity, the outlet of the mixer being represented by another cell (see Fig. 1). The latter is an absorbing state since no particle can go backwards. The process is observed for discrete moments of time with the time interval between them equal to the transition time Δt, or the duration of a transition. Let M_1 be the mass of solid particles in mixer (or in cell M_1), M_2 the mass of particles in the absorbing state (or in cell M_2), and ΔF_1 the mass of particles entering the mixer after each transition. The general Markov chain relation for representing the transition of this system between time $n \times \Delta t$ and time $(n + 1) \times \Delta t$ is therefore given by:

$$\begin{pmatrix} M_1(n+1) \\ M_2(n+1) \end{pmatrix} = \begin{pmatrix} P_{11}(n) & P_{12}(n) \\ P_{21}(n) & P_{22}(n) \end{pmatrix} \times \left[\begin{pmatrix} M_1(n) \\ M_2(n) \end{pmatrix} + \begin{pmatrix} \Delta F_1(n) \\ 0 \end{pmatrix} \right] \tag{1}$$

State 2 being an absorbing state, $P_{22}(n) = 1$ and $P_{12}(n) = 0$,and as $P_{11}(n) = 1 - P_{21}(n)$, the transition matrix only depends on the value of $P_{21}(n)$. Finally, because $M_1(n + 1) + M_2(n + 1) = M_1(n) + M_2(n) + \Delta F_1(n)$, the probabilities can be linked to measurable factors, such as the powder mass at the outlet of the mixer and the inlet flow rate $\Delta F_1(n)/\Delta t$:

$$P_{21}(n) = \frac{M_2(n+1) - M_2(n)}{M_1(n) + \Delta F_1(n)} \tag{2}$$

As long as the initial conditions, such as the initial loading mass $M_1(0)$ and the initial mass in the absorbing state, have been identified, the probability $P_{21}(n)$ can be calculated after each transition and the overall Markov chain scheme can be run. Of course, to simulate the start-up of the process, we may use: $M_1(t = 0) = M_2(t = 0) = 0$.

If P_{21} does not change with n, the chain is homogeneous and the calculation is a trivial task. But it may happen that the transition probability depends on the time elapsed, or on the state reached. In this case, the chain is non-homogeneous, or non-linear if it is also state-dependent. Actually, it is expected that the filling process of the mixer during starting will depend on the amount of powder inside the vessel until steady-state is reached. Thus, a non-homogeneous Markov chain representation would be a valuable way to represent the problem.

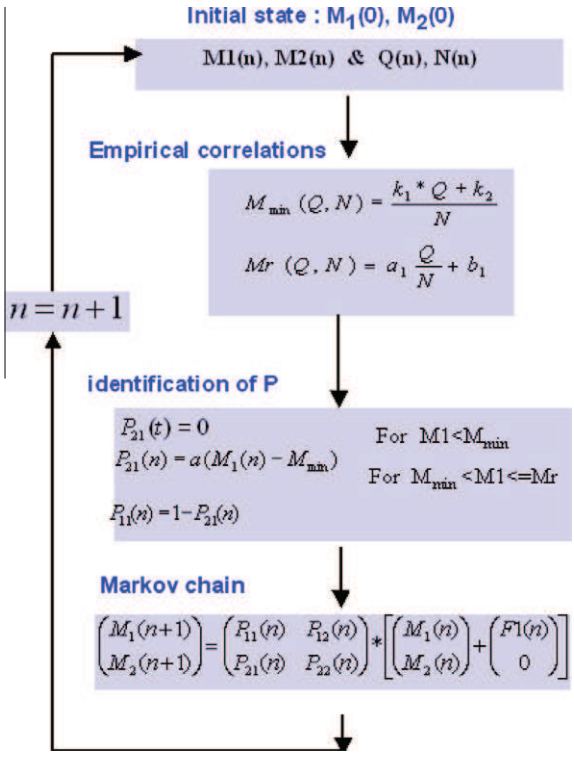

Fig. 11. Algorithm of iterative calculation for the simplified Markov chain.

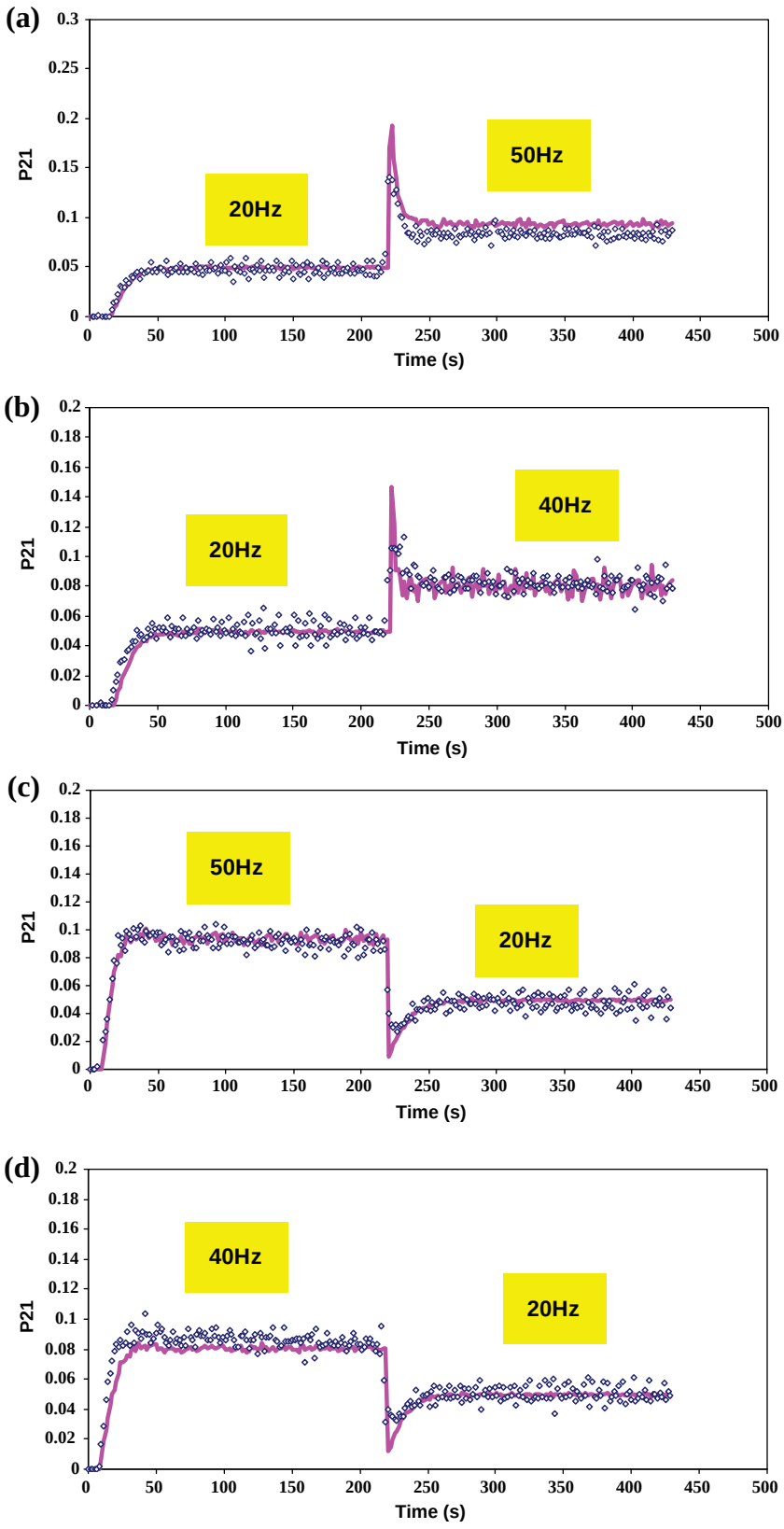

Fig. 12. Simulated (plain line) and measured (dots) time-evolution of P_{21} during step perturbation in rotational speed at $Q = 30\ kg\ h^{-1}$: (a, b) positive steps; (c, d) negative steps.

In the past, Markovian models have been applied to various powder mixers. One can refer to the following works: Chen et al. [10], Lai and Fan [11], Wang and Fan [12,13], Fan and Shin [14], Aoun-Habbache et al. [15], Berthiaux et al. [16], Ponomarev et al. [17]. As all these papers described the process under steady conditions, only homogeneous Markov chains have ever been considered

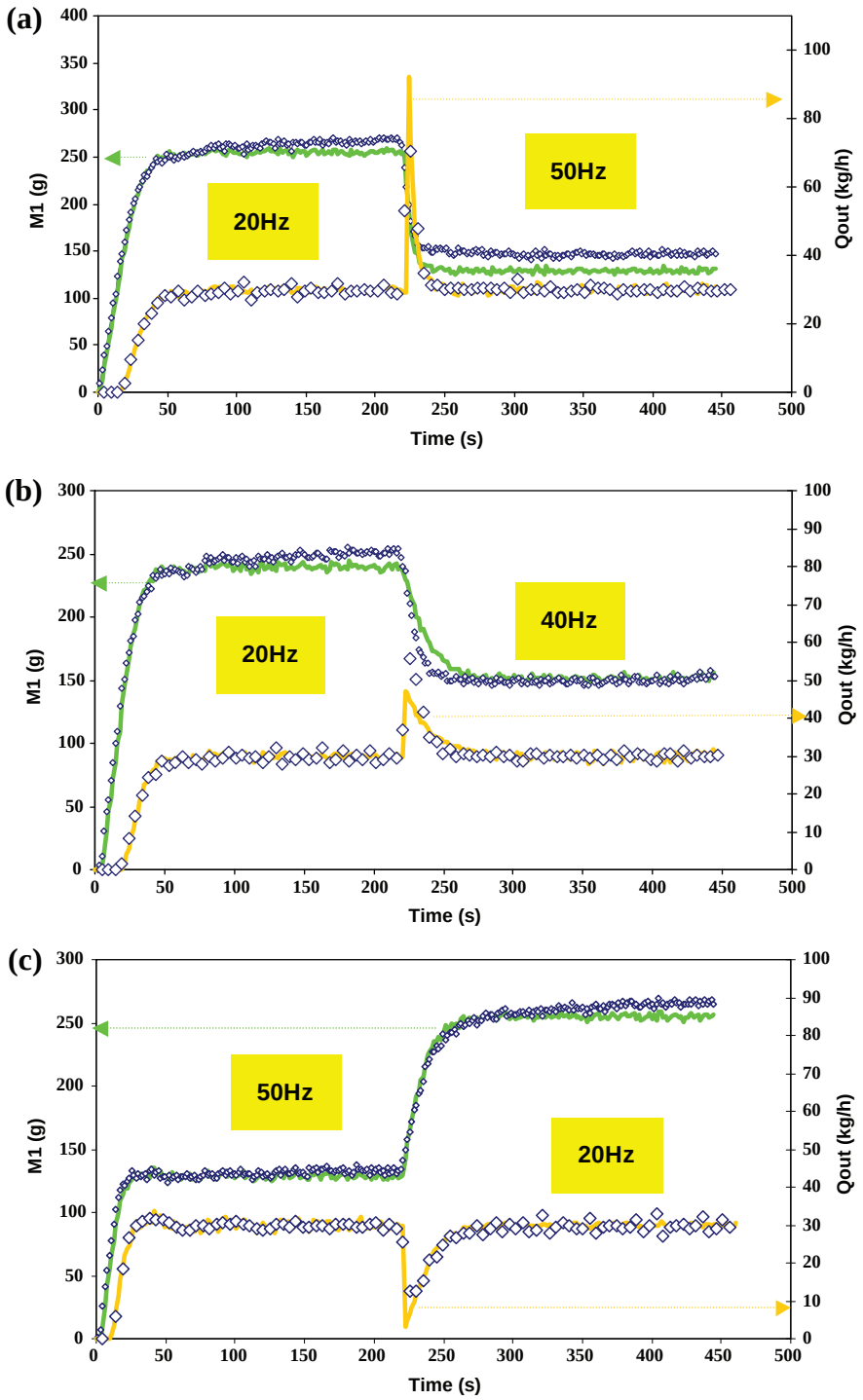

Fig. 13. Simulated (plain line) and measured (dots) time-evolution of the hold-up weight and the outflow rate during step perturbation in rotational speed at $Q = 30$ kg h^{-1}: (a, b) positive steps; (c, d) negative steps.

for mixing. Non-homogeneous chains have rarely been used for modelling since they need calculation at every step. Rippie and Chou [18] developed a Markov chain representation of a shear cell for which four different transition matrices were likely to be used, depending on the state of consolidation reached. Gyenis and Katai [19] used probability density functions instead of probabilities and introduced the concept of double stochasticity in particle flow, a concept that was examined by Mihalyko and Orban-Mihalyko [20].

3. Experimental set up and methods

The experiments were performed in a Gericke GCM 500 continuous pilot-scale powder mixer, equipped with two loss-in-weight feeders to feed the mixer with a very precise and regular dosage (see Fig. 2). Full description of the equipment can be found in Marikh et al. [21,22]. The mixer itself is a hemi-cylindrical tank of 50 cm in length, 16.5 cm in height and 20 cm in diameter (see Fig. 3A). The internal motion of the particles is due to the stirring

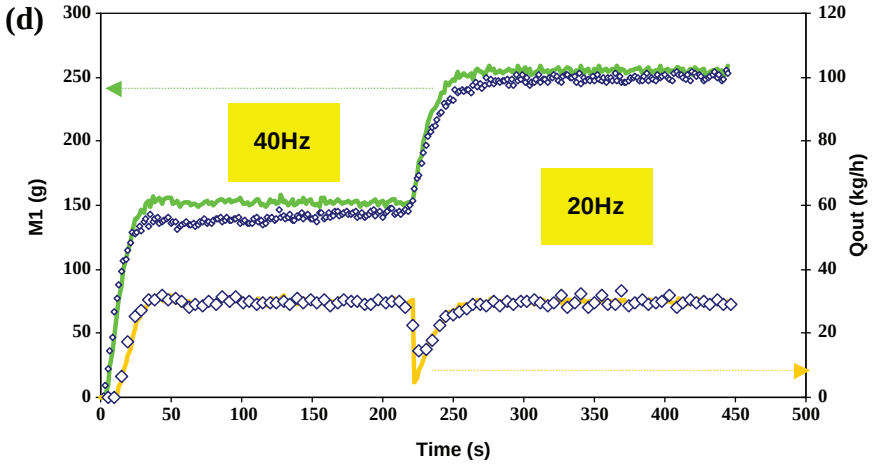

Fig. 13 (*continued*)

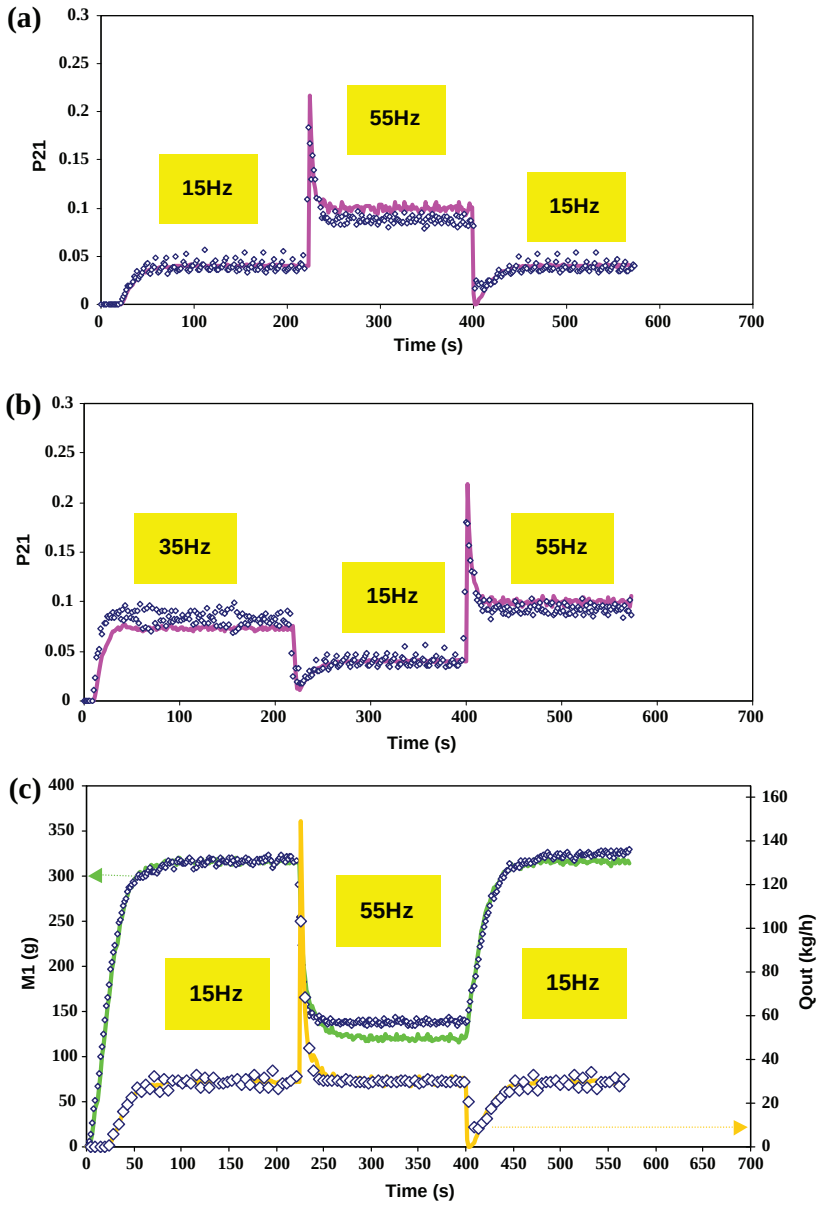

Fig. 14. Simulated (plain line) and measured (dots) time-evolution of P_{21} (a, b) and hold-up weight – outflow rate (c, d) during double step perturbation in rotational speed at $Q = 30$ kg h^{-1}.

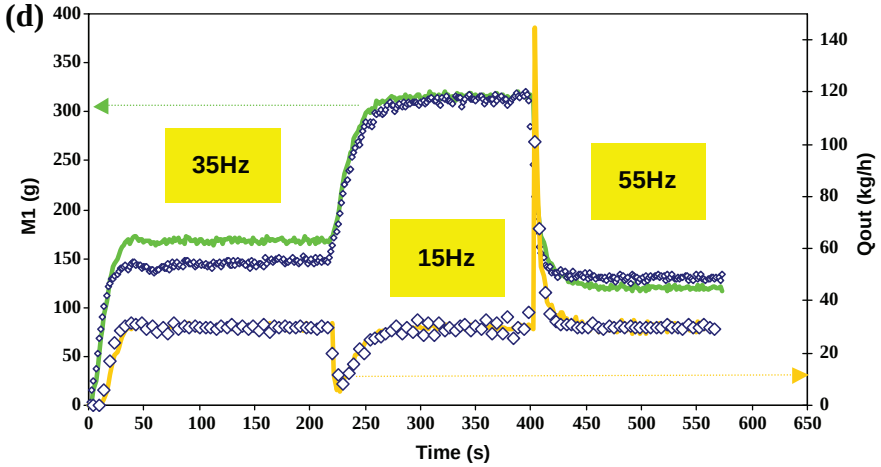

Fig. 14 (*continued*)

action of the mobile (see Fig. 3B), so this mixer can be classified in the category of convective mixers. The stirrer is constituted by 14 rectangular paddles that ensure a radial dispersion of the particles inside the vessel. An internal screw serves to transport the powder in the axial direction.

An analytical balance was placed at the outlet of the mixer, in order to measure the outflow mass in real time $M_2(t)$. As shown in Fig. 4, the change in powder mass inside the vessel, also called "hold-up weight", $M_1(t)$ can be measured indirectly by the difference between the mass introduced in the mixer and the outlet mass $M_2(t)$, in both steady and unsteady states:

$$M_1(t) = [F_1(0) - F_1(t) + F_2(0) - F_2(t)] - M_2(t) \quad (3)$$

In the above, $F_i(t)$ is the mass of particles in the hopper "i" at time t; and $F_i(0)$ is the initial mass introduced in the hopper "i". In the present work, we focus on bulk powder behaviour, so only pure particles are studied. As a consequence only one feeder is used:

$$M_1(t) = [F_1(0) - F_1(t)] - M_2(t) \quad (4)$$

All experiments were performed with food products, namely couscous particles. Table 1 gives the essential physical characteristics of this product, such as characteristic diameters, densities, as well as flowability through the determination of the Carr index. An example of the experimental evolution of the hold-up weight M_1 is given in Fig. 5. As can be seen, it increases during the start of the process in almost a linear fashion, and then becomes constant when the steady state regime is reached.

The hold-up weight M_1 is a function influenced by many variables, like the stirrer's speed of rotation N_m and the inflow rate. In the present study, the effects of these two variables on the hold-up in the mixer have been examined in the following ranges:

- For the rotational speed of the mobile N_m, which can be expressed by the frequency of the engine N: 10 20 30 40 50 Hz. The relation between N_m and the frequency of the engine was found by direct empirical observation: N_m(rpm) = 2.6 N (Hz) [21].
- For 12 different inflow rate values (Q_{in}) in the range [5–100 kg/h].

4. Results and discussion

4.1. Empirical correlations in transitory regime

As stated by Eq. (2), $P_{21}(t)$ can be determined from experimental results of $M_1(t)$. Fig. 6 gives an example of experimental results obtained for the evolution of the hold-up weight M_1 in the mixer at different rotational speeds. This example was performed with an inflow rate of 40 kg h^{-1}. As can be seen, there is a maximum value Mr. of particle mass that corresponds to the hold-up weight reached at steady state. This mass depends on the rotational speed of the stirrer and on the inflow rate used and will be linked to these process variables afterwards.

In order to determine a relation between the transition matrix P and the state of the system (M_1 and M_2), the evolution of the probability P_{21} according to the hold-up weight M_1 has been represented in Fig. 7. When examining these results, we can define three regimes of probability corresponding to the current hold-up weight in the mixer. There exists a minimum hold-up weight "M_{min}" below which no powder can flow out of the mixer, and a maximum value "Mr" above which P_{21} is constant and equal to its steady-state value ($P_{21} = P_{21max}$). When the mass M_1 is lower than M_r and higher than M_{min}, the probability P_{21} increases almost linearly with M_1. The new probability $P_{21}(n)$ depends only on the previous calculation of the states through $M_1(n)$ and both parameters (a and b) of the linear equation. In this case, the Markov chain is still not homogeneous, and the matrix must be calculated after every transition Δt.

$$\begin{aligned} &M_1 < M_{min} \quad P_{21} = 0 \\ &M_{min} < M_1 < Mr \quad P_{21}(n) = a \times M_1(n) + b \\ &M_1 = Mr \quad P_{21} = P_{21max} \end{aligned} \quad (5)$$

In the non-homogeneous regime, assuming Mr, M_{min} and P_{21max} are determined from the experiments, the parameters a and b can be determined by considering the limits of each regime: $a = \frac{P_{21max}}{Mr - M_{min}}$ and $b = -a \times M_{min}$.

This procedure allows the probability P_{21} to be calculated after every transition. However, additional empirical relations must be found to link the limits of the regimes with the operating conditions. In Fig. 8, we have plotted the experimentally obtained values of Mr. as a function of the inflow rate (Q_{in}) at different rotational speed (N). As can be seen, for a defined rotational speed N, Mr. seems to vary almost linearly with Q (the coefficient of linearity being inversely proportional to N):

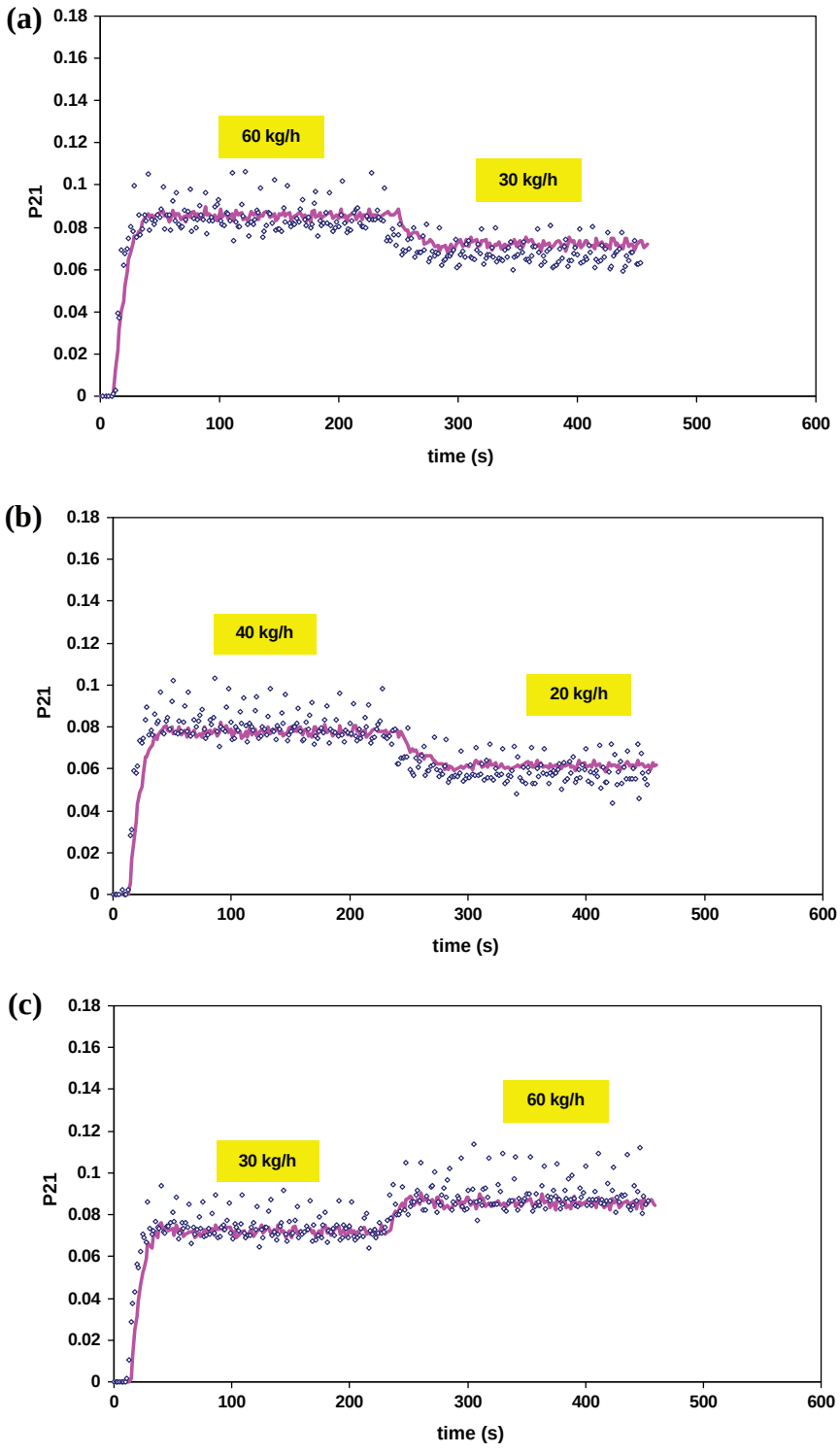

Fig. 15. Simulated (plain line) and measured (dots) time-evolution of P_{21} during step perturbation in inflow rate at $N = 30$ Hz: (a, b) negative steps; (c, d) positive steps.

$$Mr(\mathrm{g}) = a_1 \frac{Q(\mathrm{g/s})}{N(\mathrm{Hz})} + b_1 \tag{6}$$

The parameters a_1 and b_1 were identified by Levenberg–Marquardt Optimization [23] as being: $a_1 = 420$, $b_1 = 60$ g.

Another empirical correlation is proposed to link the minimal mass of particles M_{min}, from which powder starts to flow outside of the mixer during the starting up process, with operating condition (N, Q). This is presented in Fig. 9 through the experimental evolution of this minimal mass as a function of the rotational speed for different inflow rates (from 10 to 100 kg h^{-1}). From this experimental data, the following equation is proposed to predict what will be the minimal mass for a defined rotational speed N and for a defined inflow rate Q:

$$M_{\min}(g) = \frac{k_1 \times Q(\mathrm{g/s}) + k_2}{N(\mathrm{Hz})} \tag{7}$$

with $k_1 = 46$; $k_2 = 978$ g s^{-1}.

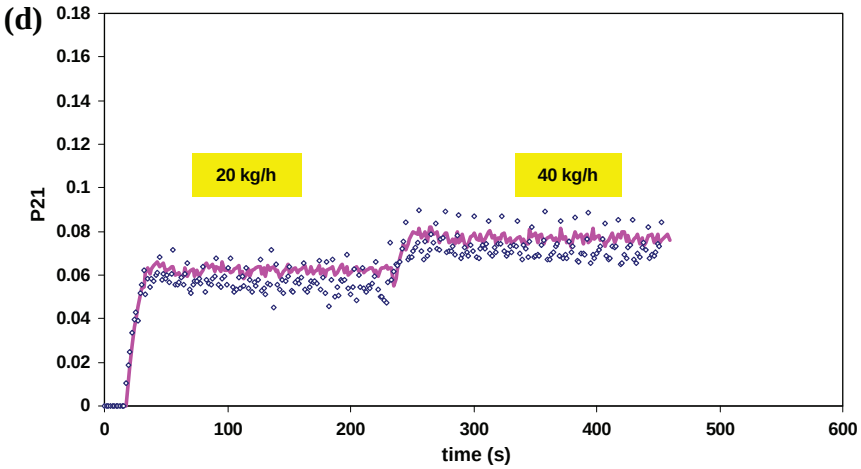

Fig. 15 (*continued*)

Finally, the probability P_{21max} can be determined using the Markov chain matrix in steady-state:

$$P_{21}(n) = P_{21max}(n) = \frac{M_2(n+1) - M_{2(n)}}{Mr(n) + \Delta F_1(n)} = \frac{Q \times \Delta t}{a1 \times \frac{Q}{N} + b1 + Q \times \Delta t} \quad (8)$$

The experimental and theoretical results of P_{21max} (calculated by Eq. (8)) are presented as a function of the inflow rates at different rotational speeds in Fig. 10. This is a first point of validation of the correlations obtained above.

4.2. Modelling strong perturbations

The aim of the present strategy is to build a framework for a general flow dynamics model capable of being used for process control. In particular, the model must be able to capture the response of the system when strong perturbations are imposed on the process variables, so as to correct a deviation in mixture homogeneity, for example.

The Markov chain can be perceived as an iterative procedure which is presented in Fig. 11. The particle mass in the mixer and the particle mass in the absorbing state must be known a priori in order to run the model. The same applies to the operating variables (rotational speed N and inflow rate Q). The empirical correlations presented above are then used to determine the minimal and the maximal hold-up weights (M_{min} and Mr). This allows the calculation of the transition probabilities at the first iteration, and then the Markov chain can be used to predict any future state of the system through the evolution of the hold-up weight in the mixer (M_1) and the real outflow rate (Q_{out}), which represents the variation of particle mass in the absorbing state M_2 between two successive transitions:

$$Q_{out}(n) = \frac{M_2(n+1) - M_{2(n)}}{\Delta t} \quad (9)$$

This method will be used to examine the response of the model to different step perturbations in terms of the stirrer's rotational speed, or the inflow rate, as compared to the experimental data.

4.2.1. Stirrer's rotational speed perturbations

Fig. 12 shows the results obtained for positive single-step perturbations (a, b), as well as for negative single-step perturbations (c, d) in terms of change in probability P_{21} against time, for a given inflow rate value. The evolution of this probability with the operational time follows the rules explained above: P_{21} equals zero until the minimum mass is reached, then it increases linearly to reach the first steady-state corresponding to the nominal set value of the rotational speed. When a positive step perturbation is applied, the transitory response of the system consists in an upward probability peak lasting approximately 20 s, before reaching the new steady-state probability value. The latter value is higher than the previous one, since increasing the rotational speed also decreases the particles' chances of staying in the mixer, which is translated in the model by Eq. (8). The same comments can be made for negative steps, except that the peak goes downwards. In the cases presented here, the Markov chain model represents the dynamics of the process in the transitory phases extremely well. Fig. 13a, b, c, d expresses the same results in terms of hold-up weight and outflow rate. The transitory evolution of the hold-up during the perturbations towards lower (positive steps) or higher (negative steps) values is respectively traduced by periods of higher or lower values of the outflow rate. This gives rise to upward or downward peaks in outflow rate, as well as in probability P_{21}, which are accurately depicted by the markovian model.

Fig. 14 shows the results obtained for two double-step perturbations on the rotational speed expressed in terms of probabilities (a, b) and hold-up weight – outflow rate (c, d). The same comments can be made as in the previous single-step perturbations. In addition, Fig. 14c allows the resilience of the process to be tested with a positive–negative step 15 Hz – 55 Hz – 15 Hz. The hold-up weight and the outflow rate obtained after the negative step are the same as before the positive step. Once again, the model is accurate in describing the dynamics of the process in transitory regimes, in particular in terms of outflow rates. This is important in the perspective of process control, as outflow rates would serve to fix the outlet homogeneity of a mixture. The relative discrepancies that can be noted for the prediction of the hold-up weights may be attributed to the recurrent nature of the Markov chain calculation, without any consequence on the outflow rate. It is worth noting that no adjustable parameter is employed in the model results presented here. The model only requires the empirical coefficients that were obtained from the start-up phase of the process.

4.2.2. Flow-rate perturbations

Single positive and negative step perturbation experiments on the inflow rate Q are reported in Fig. 15a–d at a fixed value of the stirrer's rotational speed. This type of perturbation is much less easier to perform than it is on N, for which the inertia of the command system is weaker. Important fluctuations in the experimental probability P_{21} can be seen from these graphs, but there is no

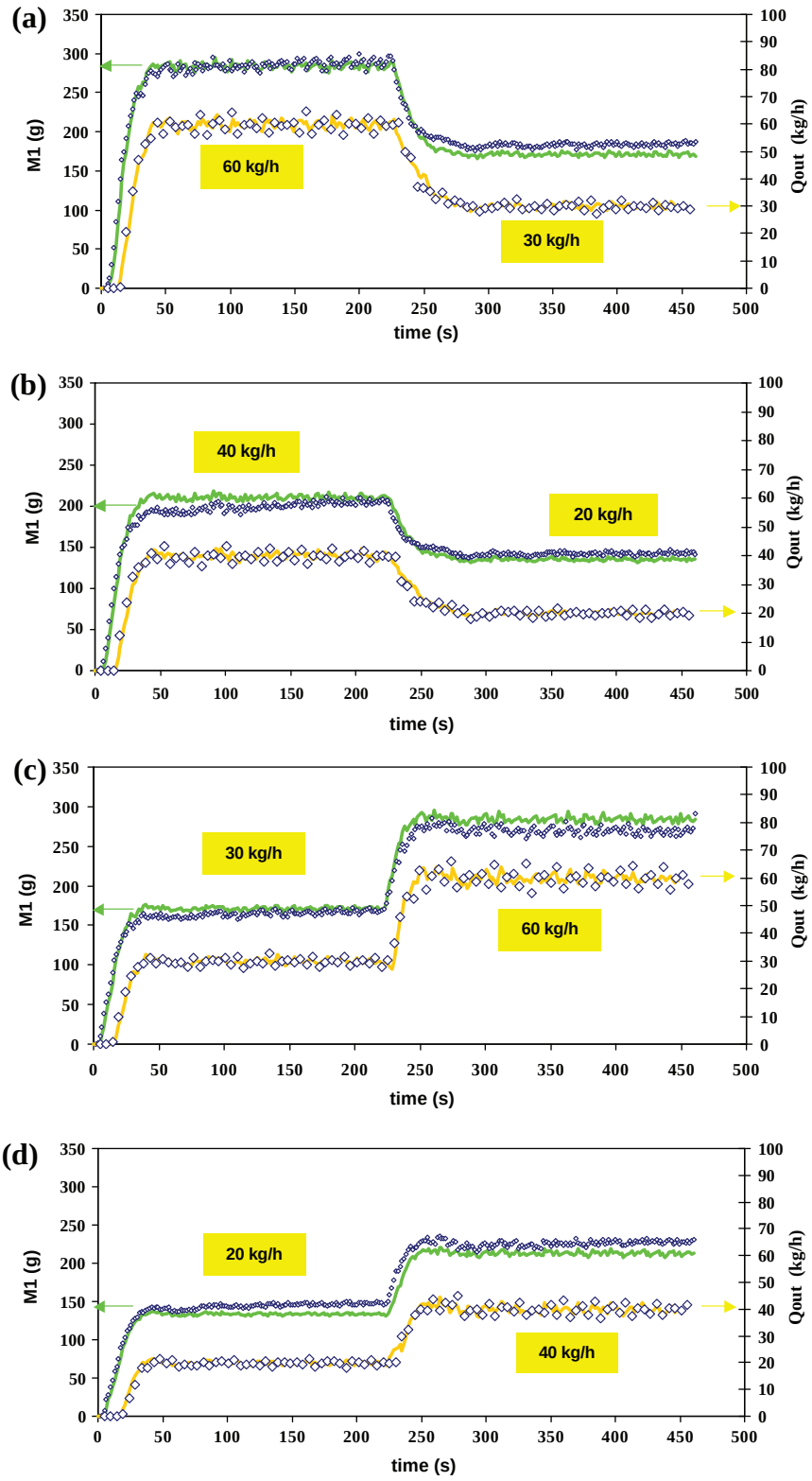

Fig. 16. Simulated (plain line) and measured (dots) time-evolution of the hold-up weight and the outflow rate during step perturbation in inflow rate at $N = 30$ Hz: (a, b) negative steps; (c, d) positive steps.

consequence on the calculation of the hold-up weights and outflow rates, which are accurately predicted by the Markov chain model (see Fig. 16).

Fig. 17 shows the modelling and experimental results obtained for double-step perturbations on the inflow rate. While there are still some discrepancies in the probability P_{21}, very good agreement is obtained for the hold-up weight and the outflow rate. As previously, the model is more predictive on the outflow rate. Fig. 17d allows the resilience of the system to be checked in terms of flow rate.

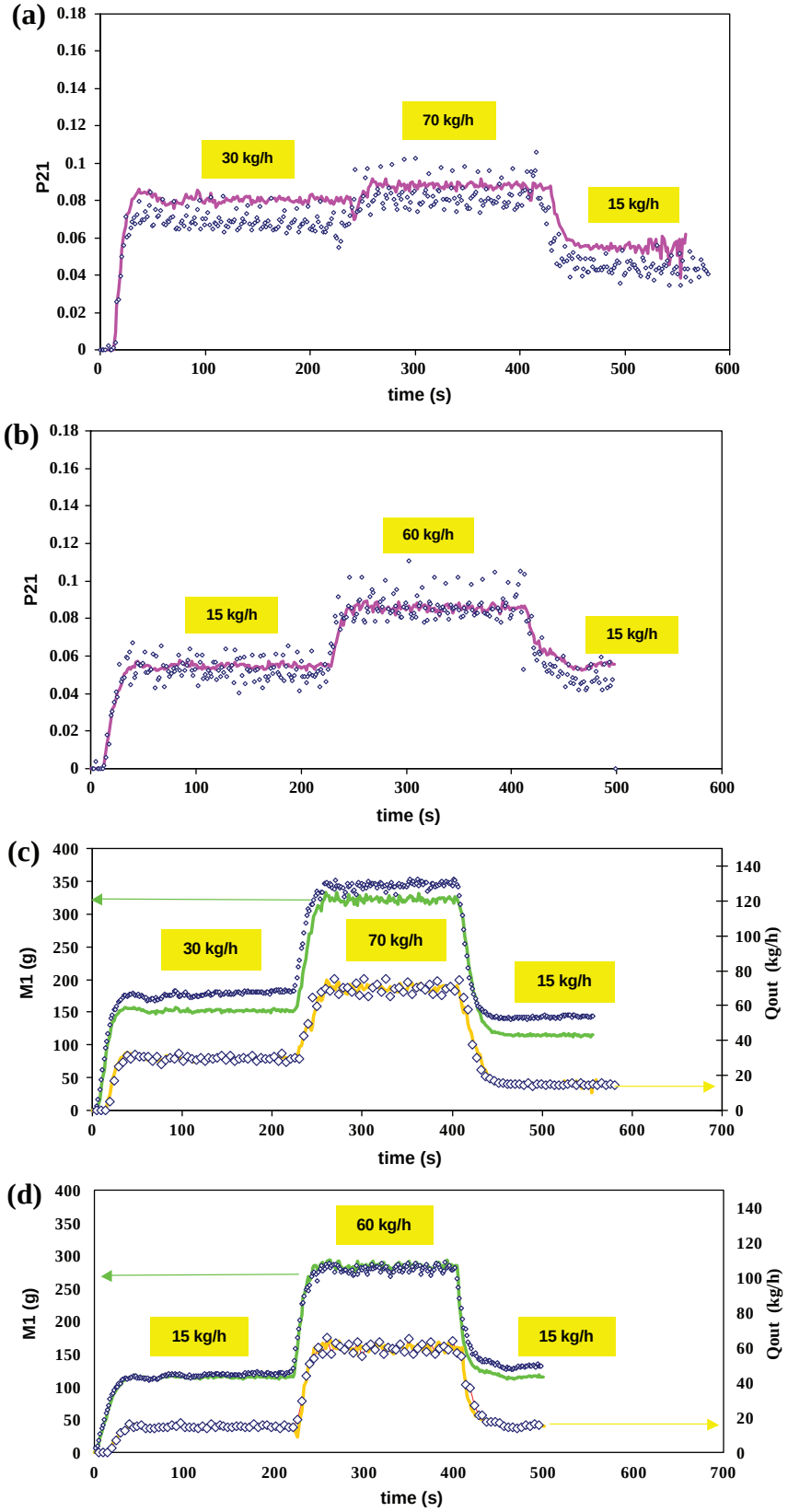

Fig. 17. Simulated (plain line) and measured (dots) time-evolution of P_{21} (a, b) and hold-up weight – outflow rate (c, d) during double step perturbation in inflow rate at $N = 30$ Hz.

5. Concluding remarks

A simple Markov chain model was developed and shown to be adequate to describe bulk particle flow dynamics in a continuous mixer. Although it is only based on the process starting characteristics, this simple model provides a full description of real outflow rate and hold-up weight in steady and unsteady states, and constitutes a first approach to process control. When the hold-up weight reaches a maximum value (Mr), a steady state regime is established according to a homogenous Markov chain. Conversely, as long as the retained mass is lower than Mr, transition matrices change at every step, and the system obeys the rules of a non-homogeneous Markov chain. The limits of these regimes are determined from the rotational speed of the stirrer and the inflow rate using empirical relations. However, the distribution of the mass of particles in the mixer and the intermediate flow rates inside the mixer are still unpredicted by the current model. As a consequence, it is not yet possible to predict the mixing of various flows related to different types of particles, such as possible particle segregation. An extension of the model presented here, which takes into account the spatial repartition of the particles in the mixer, through the discretisation of the vessel into various cells, is therefore highly desirable and will be the object of future works. Additional experiments in both steady and transitory regimes, which would result in the addition of new empirical parameters, will be performed and discussed. It is also planned to test other particulate materials, as well as mixtures of these materials. The model will again be used to provide a finer description of the particulate flows, with the sole constraint being that it is still capable of handling real-time process control.

References

[1] L. Pernenkil, T. Chirkot, C. Cooney, Continuous operation of a Zigzag blender for pharmaceutical applications, 5th World Congress on Particle Technology, Orlando, 2006.

[2] P. Portillo, M. Ierapetritou, F. Muzzio, Characterization of continuous convective powder mixing processes, Powder Technology 182 (2008) 368–378.

[3] C.A. Markley, V.M. Purri, Size segregation during mass flow – effect of deposition method and bin size, Particulate Science and Technology 17 (1999) 167–177.

[4] O.S. Sudah, D. Coffin-Beach, F.J. Muzzio, Effects of blender rotational speed and discharge on the homogeneity of cohesive and free-flowing mixtures, International Journal of Pharmaceutics 247 (2002) 57–68.

[5] R.J. Spurling, J.F. Davidson, D.M. Scott, The transient response of granular flows in an inclined rotating cylinder, Trans IChemE, 79, Part A, January 2001, pp. 51–61.

[6] H. Berthiaux, K. Marikh, C. Gatumel, Continuous mixing of powder mixtures with pharmaceutical process constraints, Chemical Engineering and Processing 47 (2008) 2315–2322.

[7] C. Ammarcha, C. Gatumel, V. Mizonov, J.L. Dirion, M. Cabassud, H. Berthiaux, Flow dynamics in a continuous mixer operating in semi-batch mode, in: 8th World Congress of Chemical Engineering, Montréal, 2009.

[8] V. Kehlenbeck, K. Sommer, A new model for continuous dynamic mixing of powders as well as in-line determination of the mixing quality by NIR spectroscopy, in: Proc. WCPT4, Sidney, 2002.

[9] H. Berthiaux, V. Mizonov, Applications of Markov chains in particulate process engineering – a review, Canadian Journal of Chemical Engineering 82 (2004) 1143–1168.

[10] S.J. Chen, L.T. Fan, C.A. Watson, The mixing of solid particles in a motionless mixer – a stochastic approach, AIChE Journal 18 (5) (1972) 984–989.

[11] F. Lai, L. Fan, Application of discrete mixing model to the study of mixing of multicomponent solid particles, Industrial Engineering Chemistry Process Design and Development 14 (4) (1975) 403–411.

[12] R.H. Wang, L.T. Fan, Axial mixing of grains in a motionless Sulzer (Koch) mixer, Industrial & Engineering Chemistry: Process Design & Development 15–3 (1976) 381–388.

[13] R.H. Wang, L.T. Fan, Stochastic modelling of segregation in a motionless mixer, Chemical Engineering Science 32 (1977) 695–701.

[14] L.T. Fan, S.H. Shin, Stochastic diffusion model of non-ideal mixing in a horizontal drum mixer, Chemical Engineering Science 34 (1979) 811–820.

[15] M. Aoun-Habbache, M. Aoun, H. Berthiaux, V. Mizonov, An experimental method and a Markov chain model to describe axial and radial mixing in a hoop mixer, Powder Technology 128 (2002) 150–167.

[16] H. Berthiaux, K. Marikh, V. Mizonov, D. Ponomarev, E. Barantzeva, Modeling continuous powder mixing by means of the theory of Markov chains, Particulate Science and Technology 22 (2004) 379–389.

[17] D. Ponomarev, V. Mizonov, H. Berthiaux, C. Gatumel, J. Gyenis, E. Barantseva, A 2D Markov chain for modelling powder mixing in alternately revolving static mixers of Sysmix® type, Chemical Engineering and Processing 48 (2009) 1495–1505.

[18] E.G. Rippie, C.H. Chou, Kinetics of mass transport in sheared particle beds: Markov chains, Powder Technology 21 (1978) 215–216.

[19] J. Gyenis, F. Katai, Determination and randomness in the mixing of particulate solids, Chemical Engineering Science 45 (1990) 2843–2855.

[20] C. Mihalyko, E. Orban-Mihalyko, A double-stochastic model of the mixing of solid particles, in: Kalman-Levy-Hubert (Ed.), Proc. CHOPS 3, The Dead Sea, June 2000, pp. 8.34–8.39.

[21] K. Marikh, H. Berthiaux, V. Mizonov, E. Barantseva, Experimental study of the stirring conditions taking place in a pilot plant continuous mixer of particulate solids, Powder Technology 157 (2005) 138–143.

[22] K. Marikh, H. Berthiaux, G. Gatumel, V. Mizonv, E. Barantseva, Influence of stirrer type on mixture homogeneity in continuous powder mixing: a model case and a pharmaceutical case, Chemical Engineering Research and Design 86 (2008) 1027–1037.

[23] D. Marquardt, An algorithm for least-squares estimation of nonlinear parameters, SIAM Journal of Applied Mathematics 11 (1963) 431–441.